Retrieving Soil Temperature at a Test Site on the Yamal Peninsula Based on the SMOS Brightness Temperature Observations

Konstantin Viktorovich Muzalevskiy and Zdenek Ruzicka

***Abstract*—In this paper, the results of radiothermal remote sensing of soil temperature at a test site on the Yamal Peninsula using full-polarimetry multiangular brightness temperature (BT) observations at the frequency of 1.4 GHz are presented. The BT data were obtained from the Soil Moisture and Ocean Salinity (SMOS) satellite with the SMOS footprint near the Polar Weather Station Marresale, the Russia Federation. The SMOS data covered the period from January 1, 2013 to December 31, 2013. The method to retrieve the soil temperature was based on solving an inverse problem by minimizing the norm of the residuals between the observed and predicted values of the BTs. The calculation of the BT was performed using a semiempirical model of radiothermal emission, which incorporated an attenuation of the microwaves in the snow pack or the canopy and a temperature-dependent multirelaxation spectral dielectric model (TD MRSDM) for an organic-rich tundra soil. The TD MRSDM was specifically designed based on laboratory measurements of the complex permittivity of the organic-rich soil samples, which were collected at the test site on the Yamal Peninsula. As a result, the values of the root-mean-square error and the determination coefficient between the retrieved and measured soil temperatures were determined to be 2.2 °C and 0.70 and 3.5 °C and 0.52, respectively, for thawed frozen soil. These results indicate the perspectives of using the full-polarimetric multiangular BT observations in the L-band for the purpose of measuring the soil temperature in the Arctic region.**

***Index Terms*—Arctic regions, microwave radiometry, moisture measurement, soil measurements, temperature measurement.**

I. Introduction

THE soil temperature in the Arctic region plays a crucial role in governing the energy fluxes between the soil and the atmosphere, thus determining the processes of permafrost degradation accompanied by carbon dioxide and methane release. At the same time, the weather station networks in the northern latitudes are too sparse to provide sufficient data on the soil temperature. Recent studies [1], [2] show that the methods of satellite remote sensing of soil temperature are promising tools to fill in the missing data of ground meteorological stations.

In [1], the values of the land surface temperature (LST) were obtained with the use of the infrared radiometer (IR) MODIS and compared with the values of the ground surface temperature (GST) measured *in situ* by meteorological stations at a depth of 3–5 cm. The observations were conducted over 12 test sites during the period of 2000 to 2008 in the northern territories of the U.S. and Canada. The obtained values of the LST deviated from the *in situ* measured values of the GST by 4.4 to 14.7 °C in terms of root-mean-square error (RMSE), and the determination coefficient (R^2) varied in the range of 0.49–0.92. One of the primary factors limiting the use of IR for measuring the GST is cloud cover, and, according to Hachem *et al.* [1], approximately 40% of MODIS observations were accompanied by dense clouds. Due to the short wavelength, IR measures the temperature of the apparent surface of land (bare soil, vegetation, or snow), and the LST values from MODIS are better correlated with the air temperature (0.98) than with the GST (0.62) [1].

A more promising tool, in terms of avoiding cloud interference and wave penetration depth, is the application of microwave radiometers. In [2], the values for the effective ground surface temperature (EGST) were obtained with the use of the advanced microwave scanning radiometer-EOS (AMSR-E) microwave radiometer using the frequency range from 6.9 to 89 GHz and compared with the values of the GST measured *in situ* by the meteorological stations in the topsoil layer at 0–8 cm. The observations were conducted over seven test sites located in the northern territories of the U.S. and Canada during the periods of 2002 to 2004. For the nonforested sites, the obtained values of the EGST deviated from the values of *in situ* measured GST by 2.2 to 10.5 °C in terms of RMSE, and R^2 varied in the range 0.24–0.77. The sensing depth of the AMSR-E observations was limited by 0.5–2.8 cm in the case of a thawed bare soil, as was noted in [2], and may not exceed 6 cm in the case of frozen bare soil, according to Zhao *et al.* [3]. Because the canopy and snow pack affects the sensitivity of the microwave remote sensing of soil temperature in the microwave band of the AMSR-E (6.9–89 GHz), applying a lower frequency may reduce these affects and increase the accuracy of the soil temperature retrieval.

A theoretical feasibility study to retrieve the soil temperature with the use of multiangular brightness temperatures (BT) at 1.4 GHz in the area of northern Alaska was recently conducted in [4]. In the course of studies in [4], the BTs were simulated, as if they were measured by the Soil Moisture and Ocean Salinity (SMOS) satellite with a microwave imaging radiometer using an aperture synthesis (MIRAS) radiometer. For this purpose, the bare soil emissivity model suggested in [5] and the temperature-dependent dielectric model of organic-rich Arctic soil [6] were used. In addition, the data on soil moisture, soil dry bulk density,

Manuscript received October 02, 2015; revised March 12, 2016 and January 16, 2016; accepted April 07, 2016. Date of publication June 07, 2016; date of current version July 05, 2016. This work was supported by the Russian Science Foundation under Project 14-17-00656. *(Corresponding author: Konstantin Viktorovich Muzalevskiy.)*

The authors are with the Kirensky Institute of Physics, Krasnoyarsk 660036, Russia (e-mail: rsdkm@ksc.krasn.ru; tramtara@seznam.cz).

Color versions of one or more of the figures in this paper are available online at http://ieeexplore.ieee.org.

Digital Object Identifier 10.1109/JSTARS.2016.2553220

and soil temperature measured by the Biosphere Station Franklin Bluffs (69°39′N, 148°43″W) from 1999 to 2001 were employed. Based on the simulated angular patterns of the BTs, as if taken from the SMOS radiometer, the surface soil temperature and the temperature gradient were retrieved by minimizing the residual norm between the simulated BTs and those calculated with the simplified radiothermal model, as outlined above. The approach of Mironov *et al.* [4] needs to be tested in real conditions to clarify its principal applicability to derive the soil temperature using SMOS BT observations. In this paper, the methodology developed in [4] was applied to determine the soil temperature at the test site on the Yamal Peninsula based on the SMOS multiangular BT patterns.

II. Test Site and Data

A. Test Site and In Situ Data Measurements

The area next to the Weather Station Marresale (WS) on the coast of the Kara Sea, Yamal Peninsula was selected as a test site. The coordinate of WS is (69.7151N, 66.8209E). The MODIS optical image of the test site is depicted in Fig. 1. This is a false-color composite (RGB = bands 2, 2, and 1), from a surface reflectance daily MYD09GQ product (250-m resolution) showing a portion of the tiles of h20v01 and h20v02 over Yamal Peninsula acquired on August 4, 2015.

This choice is due to the following two factors. First, the temperature-dependent dielectric model previously developed in [7] and [8] is based on the soil samples collected at the area of the weather station Vaskiny Dachi (see Fig. 1), proximate to the test site. Second, the average daily soil temperature (WS-ST) and air temperature, measured at a height of 2 m above the ground for every third hour during the day, are readily available from WS [9], [10], and the SMOS radiometric data. Based on the five points of the WS grid, primarily Marresale No. 1, No. 3, No. 6, No. 17, and No. 43, separated by a distance of 100 m, the average WS-ST (WS-AST) was calculated and used for comparisons with the retrieved soil temperatures. WS-ST was measured at the soil surface.

The landscape at the area of the test site is a typical tundra, which is covered by nontussock sedge, moss, lichens, and dwarf shrubs with heights less than 40 cm. The area within the test site was occupied by soils covered with vegetation (92.4%) and open water bodies (7.6%). The vegetation cover was comprised of areas of erect dwarf-shrub (22.3%), a low-shrub tundra (56.2%), nontussock sedge, dwarf-shrub, and moss tundra (14.9%). These data were obtained on the basis of electronic vegetation and water maps of the Yamal Peninsula from the Institute of Arctic Biology of the University of Alaska [11]. For the area of the test site, the maximum vegetation biomass from July 6 to September 28, 2013 was equal to 0.36 kg/m^2, which was calculated on the basis of the NDVI index (two-week product of MODIS MOD13Q1). On the test site area, sand and sandy-loam soils predominate in the near surface (0–30 cm) of the active layer [12] and have the following percentages by weight: sand 36.7%, silt 50.1%, and clay 13.2% (averaged values) [13]. To further study the soils in the area of the test site at three different locations (see Fig. 1), 20 soil samples were collected. In the areas of the weather station Marresale, the Bovanenkovo oil and gas field, and the weather station Vaskiny Dachi, three, seven, and ten soil samples, respectively, were collected in the form of cylindrical columns 25 cm in height and 10 cm in diameter. Each soil sample was collected from a different type of the landscape (on the hills and in the valleys of lakes and rivers, in wet and dry tundra, in bare soil and in soils covered with different of vegetation, etc.). The upper horizon of the collected soils contained plants with half-rotten organic material with mineral soil particles, and the thickness of the layer varied from 2 to 25 cm. The lower portion of the soil samples was formed of mineral soils. The average thickness of the organic upper layer of soil samples was found to be on the order of 10 cm. The average soil dry bulk density of the organic upper layer of soil samples was found to be on the order of 0.3 g/cm^3. Based on the fact that the topsoil is the most significant in the microwave emission of a bare soil during modeling, we assumed that the active layer of the soil was composed of an organic-rich soil. A detailed description of the organic-rich soil sample, which was selected to create the dielectric model, is described in Section III-B. The depth of seasonal thaw of the soil varied from 0.4 to 0.75 m (polygonal peatlands) to upward of 1.5–1.8 (nonvegetated sands) [12]. The elevations were uniformly low ($<$90 m) across the Yamal Peninsula [14], and on the test site, elevations were approximately 40 m [12].

B. SMOS BT Data

The two-dimensional (2-D) interferometric radiometer on board the SMOS measures the BT of the earth surface at vertical and horizontal polarizations in the range of viewing angles from 0° to 65° with a space resolution of 43 km × 43 km [15]. This product is a daily-averaged product and includes all the BTs acquired during that day, separately for ascending and descending orbits, transformed to a ground polarization reference frame and averaged into fixed classes of the viewing angle with values in the range of 0°–65°. SMOS has a sun-synchronous orbit such that at ∼6 A.M. (local time), the SMOS is ascending (the satellite is moving from south to north), and at ∼6 P.M., the SMOS is descending (the satellite is moving from north to south). In this paper, for the SMOS observations from January 1, 2013 to December 31, 2013, SM_CLAS_MIR_CDF3A, the CATDS product (ascending orbit) with the coordinate closest to WS was selected. The ascending SMOS orbit was selected following studies [17]–[19], in which at ∼6:00 A.M. (local time) the vertical profiles of the soil temperature and the soil dielectric properties were likely to be more uniform than at other times of the day. This early morning condition minimized the difference between the canopy and soil temperatures and the thermal differences between the land cover types within a pixel. These factors minimized the soil moisture and temperature retrieval errors originating from the use of a single effective temperature to represent the near surface soil and canopy temperatures [17]. In the period of observations, the average radiometric accuracy of the SMOS BTs data was ∼6 K in the entire range of viewing angles and for both the H- and V-polarizations. These estimates were based on the data block «Pixel_Radiometric_Accuracy»

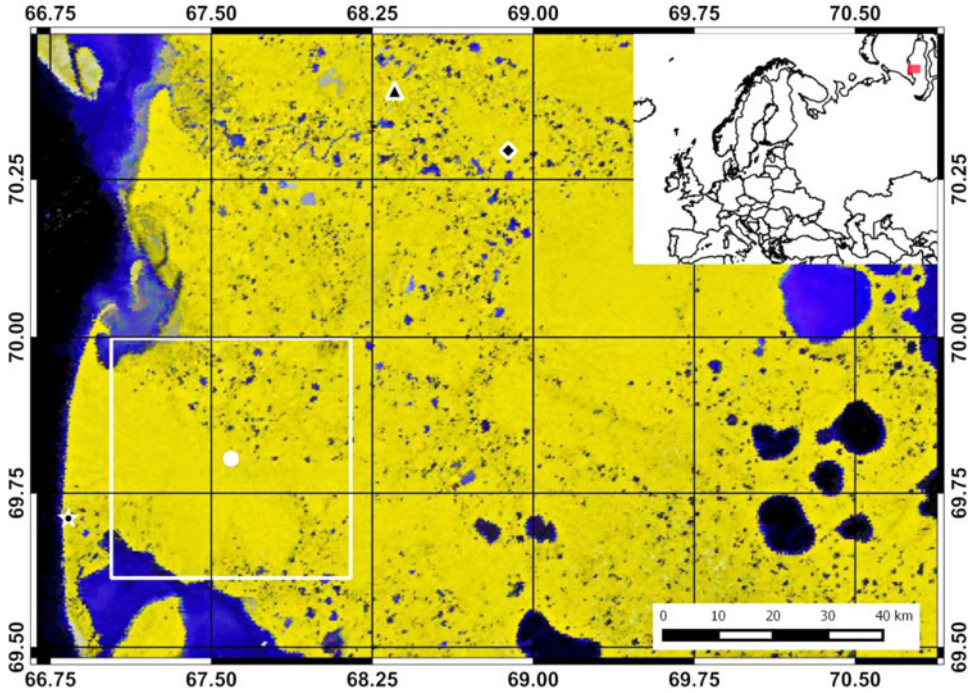

Fig. 1. Images of the test site area in different scales. On a main panel, region of the test site is schematically depicted as a square (SMOS pixel) with white edges, length of 43 km. Coordinate of the central point of the pixel is (69.8057N, 67.5913E). Symbols of the asterisk, triangle, and diamond on the main panel are shown locations of soils sampling at areas of Marresale weather station, Bovanenkovo's oil and gas field (70.3897N, 68.3540E), and Vaskiny Dachi weather station (70.2955N, 68.8835E), respectively.

of the SMOS product. The SMOS multiangular BT (CATDS product) in the range of viewing angles from 0° to 60° obtained from 1 to 10 data points. From 365 available observations, only 136 were processed. The remaining data were discarded during processing because 1) the relevant data included an angular interval less than 10°, and over the entire range of viewing angles, only 1–2 data points were contained; therefore, the retrieval algorithm did not converge, or 2) the BT model predicted the measured angular dependencies with an RMSE of more than the radiometric accuracy of the SMOS measurements.

Given that this study used only the ascending orbit (6 A.M.), it is necessary to estimate the additional error that could occur when comparing the average daily soil temperature, measured by a meteorological station, with the soil temperature, retrieved from a single SMOS observation [from the original ESA database of SMOS images, the satellite observations at the ascending orbit of the test site performed one time at approximately 8 A.M. (local time)]. Such estimation can be made on the basis of air temperature data. The comparison result of the average daily air temperature with the air temperature at 8 A.M. (local time), which were measured by the weather station Marresale, is shown in Fig. 2. The data, presented in Fig. 2, were obtained from January 1 to December 31, 2013 from the catalog of the NOAA's National Centers for Environmental Information [10], and the index Nbr of the weather station is 23 032. In this regard, we assumed that the comparison of the average daily soil temperature with the soil temperature retrieved from radiometric observations at the ascending orbit is justified within the error of 2.6 C.

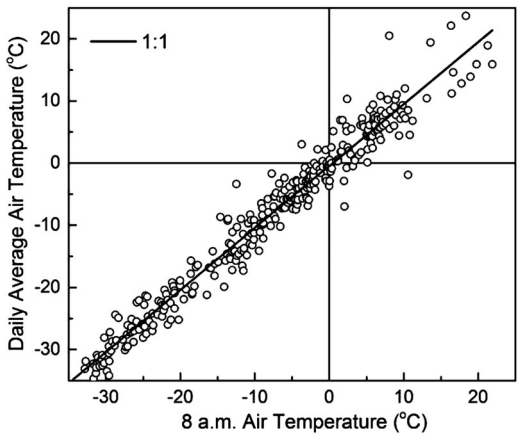

Fig. 2. Correlation between average daily air temperature and 8 A.M. air temperature. RMSE and R^2 values were determined to be 2.6 °C and 0.96, respectively.

C. SMOS/MIRAS and GCOM-W1/AMSR2 Soil Moisture, MODIS LST, and GCOM-W1/AMSR2 Snow Depth Products Over the Test Site

In the absence of ground-truth measurements of the soil moisture during 2013 at the test site, the SMOS/MIRAS and GCOM-W1/AMSR2 soil moisture standard products were used as independent additional data (see Fig. 3). The values of the SMOS/MIRAS soil moisture were acquired from the CATDS L3SM one day product (SM_CLAS_MIR_CLF31A) for the ascending (6 A.M.) orbit [16]. Values of the GCOM-W1/AMSR2

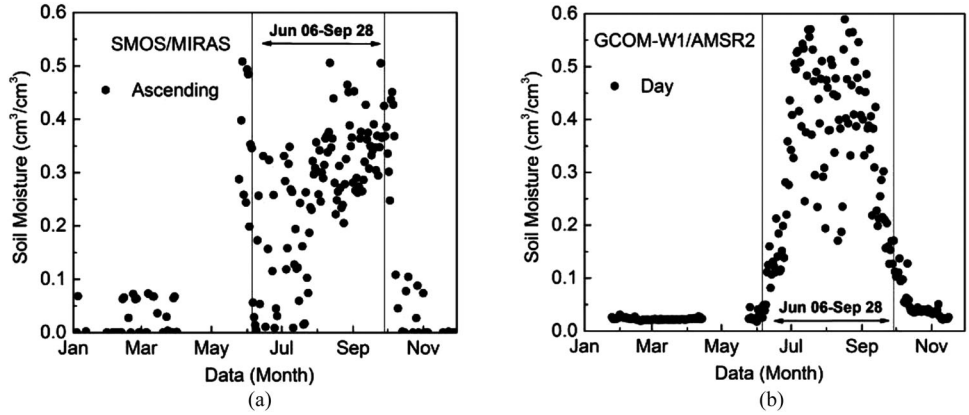

Fig. 3. Temporal variation of soil moisture during 2013, at the test site according to the (a) SMOS CATDS L3SM one day product (SM_CLAS_MIR_CLF31A) for ascending (6 A.M.) orbit and (b) GCOM-W1/AMSR2 L2 SMC day (descending orbit 1.30 A.M.) product. Vertical solid lines indicate period from June 6 to September 28, 2013, for which average daily soil temperatures, measured by WS *in situ*, were positive.

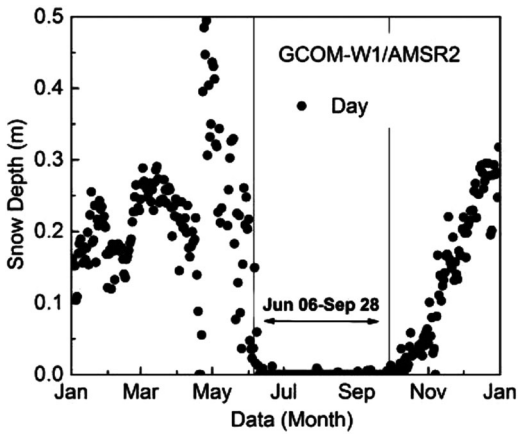

Fig. 4. Temporal variation of snow depth, during 2013, at the test site according to GCOM-W1/AMSR2 L2 SND day product.

soil moisture were acquired from the GCOM-W1/AMSR2 L2 SMC day (descending orbit 1.30 A.M.) product [20].

According to the SMOS data [see Fig. 3(a)], the mean and standard deviations of the soil moisture were determined to be 0.27 ± 0.14 cm^3/cm^3. According to the GCOM-W1/AMSR2 data [see Fig. 3(b)], the mean and standard deviations of the soil moisture were determined to be 0.33 ± 0.15 cm^3/cm^3. The soil moisture values obtained by the satellites have a mean value and standard deviation typical of the Arctic tundra. Nonetheless, these values may diverge from the *in situ* values measured in the topsoil layer of 0–20 cm by a factor of 2 to 3 [21].

For additional information about the thickness of the snow pack, GCOM-W1/AMSR2 L2 SND day products (see Fig. 4) were used. The vertical solid lines in Figs. 3 and 4 indicate the period from June 6 to September 28, 2013, when WS was positive. On average, the snow depth was approximately 0.15 m (see Fig. 4). However, as shown in [22], the propagation effects must be taken into account in dry snow in the L-band, nevertheless further at modeling, we neglected the scattering and refraction of microwaves in the snowpack and canopy for the simplicity of the model and for a transparent analysis. However, the absorption of the emission in the snowpack or vegetation, which originated from the underlying soil, was accounted with the help of the widely used τ–ω model [22], by introducing a parameter of optical thickness. This model calculates the approximate BT of the layered structure, consisting of soil covered with vegetation or snowpack. A more detailed description of the model is provided in Section III-A. From April 20 to June 5, there was a significant increase in the snow depth (see Fig. 4) that may impact the accuracy of the BT modeling without taking into account the scattering and refraction of microwaves in the snowpack.

MODIS data have been used successfully to measure bare soil temperatures, but in a number of studies in the Arctic territories, the MODIS LST product experienced a substantial error with respect to ground-truth soil temperature measurements [1], [23]–[25]. As in [1], we also observed that for the test site, the MODIS LST had a better agreement with air temperature (2 m above the ground) rather than with the surface soil temperature. Combining the day and night products, V041 MODIS LST L3 Global 1 km (MOD11A1 and MYD11A1) were used to calculate the average LST per day in the coordinate of the center of the SMOS pixel. A comparison between the MODIS LST and air temperature, MODIS LST and WS-AST have shown a higher correlation of the MODIS LST with the air temperature than with the WS-AST (see Fig. 5).

The determination coefficient and RMSE were determined to be 0.88 and 4.72 °C for (MODIS LST/air temperature) and 0.38 and 7.58 °C for (MODIS LST/WS-AST), respectively. Because the IRs are the primary satellite instruments used for LST measuring, and based on the data [1], [23]–[25], as well as our results, we conclude that the development of the satellite methods for soil temperature measurements with a higher precision is still a challenge for the Arctic regions. In the following sections, a BT model and a method of the soil temperature retrieval based on the SMOS data are presented.

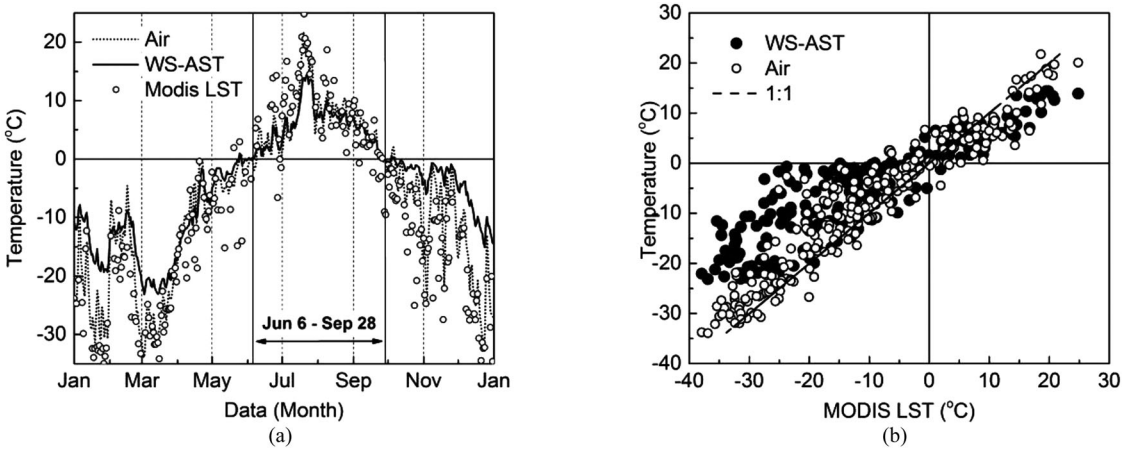

Fig. 5. Comparison between average daily soil temperatures measured at five *in situ* sites (WS-AST) and average MODIS LST values on the test site by combining day and night MODIS products (V041 MODIS LST L3 Global 1km) during 2013 year. (a) Time series and (b) correlation between these values. The calculated RMSE are 4.72 and 7.58 °C, respectively, for MODIS LST versus air temperature and MODIS LST versus WS-AST. The calculated determination coefficient are 0.88 and 0.38, respectively, for these cases.

III. Microwave BT Model of Arctic Soils

A. H–Q Semiempirical Emission Model

To model the BT, $T_{B,P}^{\mathrm{th}}(\theta)$ as a function of the viewing angle θ for the horizontal $p = H$ and vertical $p = V$ polarizations, we used a semiempirical model for microwave emission introduced in [26] and further developed the case of bare soil in [27]

$$T_{B,P}^{\mathrm{th}}(\theta) = \left(1 - \left[(1-Q)\left|R_P(\theta,\varepsilon_s)\right|^2 + Q\left|R_q(\theta,\varepsilon_s)\right|^2\right] \times e^{-H_r \cos^N\theta - 2\tau/\cos\theta}\right) \cdot T_s. \quad (1)$$

Combinations $p = H$, $q = V$, and $p = V$, $q = H$ are possible. Here, T_s is the physical soil temperature; $R_p(\theta, \varepsilon_s)$ is the Fresnel reflection coefficient; $Q = 0.118H_r$ is the depolarization factor, which accounts for the polarization mixing effects; $N = 1.615[1 - \exp(-H_r/0.359)]$ and H_r are the parameters that modify the angular dependence of the BTs due to the roughness of the soil surface; and ε_s is the soil complex permittivity. In the model (1), the influence of the snowpack and vegetation on the BT is simplistically taken into account by an absorbing layer, the attenuation of microwaves, which is characterized by the optical depth at the nadir τ. The vegetation and snowpack temperatures were assumed to be the same. The model (1) does not take into account the effects of scattering caused by the snowpack and vegetation. The largest error 6.5 K of the model (1), at $\tau = 0$, was estimated from the experiments [27] conducted with predominantly mineral soils in thawed conditions, at only one specific location (PORTOS 1993 data set, Avignon, France). The model (1) can give significant errors, without taking into account the scattering and refraction of microwaves in the snowpack and vegetation, particularly when they become wet. In the off-season, we did not take into account the layers of thawed and frozen soil emerging at the surface. In addition, the model (1) does not incorporate the relief and slopes of the test site because the test site elevations do not exceed ∼40 m, and such a simplification [28] of the relief causes an error of the order of 0.1–2K, which falls within the limits of the SMOS brightness measurement error. The model (1) does not account the effect of water bodies on the radiobrightness temperature in the SMOS footprint. This disregard is the source of the error for the determination of the soil temperature. However, as has been shown in the field experiment [29] over Australia, the tolerable thresholds of water fractions in the range from 0.02 to 0.08 for achieving a maximum 4 K underestimation in the BT were found. Therefore, within the error of 4 K, which is within the limits of error of the model (1), we missed the influence of water bodies. The values of the model parameters within the pixel sensing were spatially invariable. This is the average value, which corresponds to the integrated BT of the entire SMOS pixel. Finally, the vertical profiles of soil moisture, temperature, and permittivity were not taken into account in the model (1) because we assumed that when we used the ascending SMOS orbit, these profiles were more uniform in depth [17]–[19]. Estimates in the L-band show that the penetration depth of microwaves can reach up to 12 cm in the case of relative dry soil (0.1 cm^3/cm^3) [18], while the BTs reach their saturation values at a frost depth up to 10 cm (theory) and 30 cm (experiments) [30]. Due to this fact, we assumed that to form a microwave emission, the organic soil horizon (the thickness was approximately 0.1 m at the test site) was more essential than the subjacent mineral horizon of the soil. Therefore, in the model (1), we assumed the soil to be vertically homogeneous and consisting of only an organic layer. To calculate the BT in the model (1), the permittivity model for arctic tundra organic-rich soil [7], [8] was used.

B. Permittivity Model of Arctic Tundra Soil

To develop a soil temperature-dependent multirelaxation spectral dielectric model (TD MRSDM) [7], [8], soil samples were collected at the area of the weather station Vaskiny Dachi close to the test site (see Fig. 1). The sample was extracted

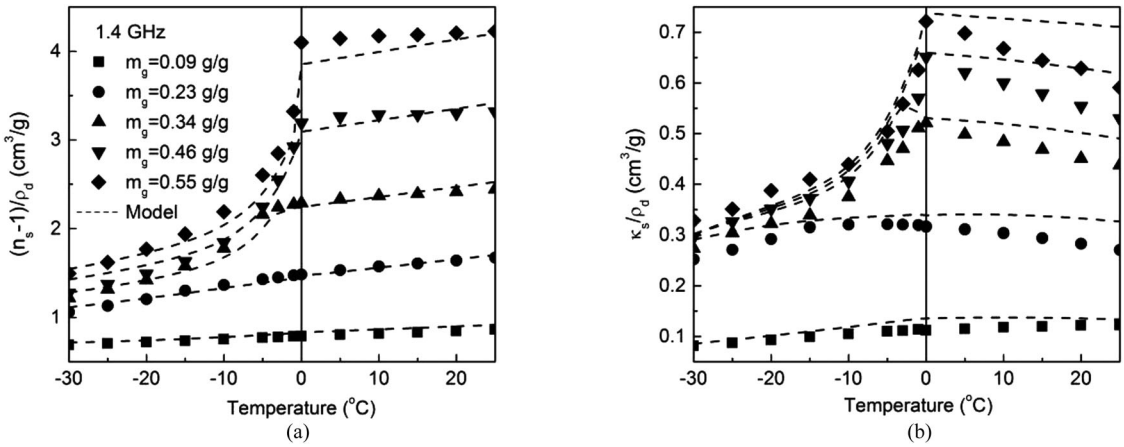

Fig. 6. (a) Behavior of the reduced refractive index and (b) normalized attenuation coefficient versus temperature, with varying values of gravimetric moisture, at the frequency of 1.4 GHz. The measured and modeled data are shown with symbols and dashed lines, respectively.

from the organic layer at depths of 9 to 14 cm and consisted of mineral solids and decomposed organic matter. In vivo, the air dry bulk density of the sample equaled 0.26 g/cm^3. During measurements in a coaxial container, the dry bulk density varied from 0.72 to 0.87 g/cm^3. The percentages of organic matter and mineral solids components were as follows: organic matter $\sim$50%, quartz $\sim$30%, potassium feldspar $\sim$5–10%, plagioclase $\sim$5–10%, and chlorite, mica, smectite in trace amounts ($<$1%). The procedures for soil sample processing, dielectric measurements, and regression analysis for developing TD MRSDM are provided in [6], [31]. The TD MRSDM enables the calculation of complex permittivity for the given organic-rich soil as a function of soil dry density ρ_d, gravimetric soil moisture m_g, wave frequency f, and temperature T_s. The TD MRSDM ensures predictions of the real and imaginary parts of complex permittivity in the ranges of $0.03\ \mathrm{g/g} < m_g < 0.55\ \mathrm{g/g}$, $-30\ ^\circ\mathrm{C} < T < 25\ ^\circ\mathrm{C}$, and $0.05\ \mathrm{GHz} < f < 15\ \mathrm{GHz}$. The validation of this model demonstrates good agreement with the measured data. The values of the determination coefficient for the real and imaginary parts of complex permittivity were determined to be 0.997 and 0.991, respectively. The estimates of the RMSE of the predicted values relative to the measured values yielded 0.348 and 0.188 in the cases of real and imaginary parts of complex permittivity, respectively [7], [8]. These error estimates were in the order of that available for the soil dielectric measurement itself. However, in the frequency range of 1–3 GHz, the maximum differences between the measured and modeled values of complex permittivity were observed [7]. The predicted with the TD MRSDM and measured values of reduced refractive index $(n_s - 1)/\rho_d$ and normalized attenuation coefficient κ_s/ρ_d at the SMOS frequency of 1.4 GHz are shown as a function of temperature and moisture in Fig. 6. The refractive index and the normalized attenuation coefficient was determined by the following equation: $n_s^* = \sqrt{\varepsilon_s} = n_s + i\kappa_s$, where i is the imaginary unit and n_s^* is the complex refractive index.

As seen in Fig. 6, the refractive index and the normalized attenuation coefficient were strongly dependent on soil moisture and weakly dependent on soil temperature, in the case of thawed soil. In the case of frozen soil, when the soil moisture was $m_g > 0.34$ g/g, the refractive index and the normalized attenuation coefficient strongly depended on the soil temperature and weakly depended on the soil moisture. The sensitivity to soil moisture of the refractive index and the normalized attenuation coefficient increased only when the soil temperature was approximately zero (-3–0 °C). Taking into account the features of behavior of the refractive index and the normalized attenuation coefficient (see Fig. 6), it is possible to propose the following approaches for soil moisture and temperature obtained from the radiothermal observations.

IV. Method for Retrieving of Soil Temperature

According to (1) and the soil permittivity model [7], the BT $T_{B,p}^{\mathrm{th}}(\theta)$ can be presented as a function of the following parameters: $T_{B,p}^{\mathrm{th}}(\theta) = T_{B,p}^{\mathrm{th}}(\theta, \rho_d, m_g, T_s, H_r, \tau)$. To reduce the numbers of the parameters to be retrieved, the dry bulk density was set equal to the mean dry bulk density, $\rho_d = 0.32$ g/cm^3, of the topsoil layer at 0–6 cm, which was measured *in situ* at the area of the weather station Marresale, the Bovanenkovo oil and gas field, and the weather station Vaskiny Dachi.

The method to retrieve the soil temperature was based on solving an inverse problem by minimizing the norm of the residuals between the observed $T_{B,p}^{m}(\theta_i)$ and predicted $T_{B,p}^{\mathrm{th}}(\theta_i)$ values of BTs

$$F = \sum_{p=H,V} \sum_{i=1}^{N} \left| T_{B,p}^{m}(\theta_i) - T_{B,p}^{\mathrm{th}}(\theta_i) \right|^2 \qquad (2)$$

where N is the total number of viewing angles in the range of $0^\circ \leq \theta_i \leq^\circ 60$. Because the soil permittivity, and hence, the soil emissivity, of thawed soil weakly depends on the soil temperature and strongly depends on the soil moisture (see Fig. 6), at the first step, the soil moisture was.When minimizing the norm (2), the soil temperature and the optical depth were set as a constant equal to air temperature and zero, respectively, and the roughness parameter was retrieved. At the second step, when minimizing the norm (2), the roughness parameter, optical

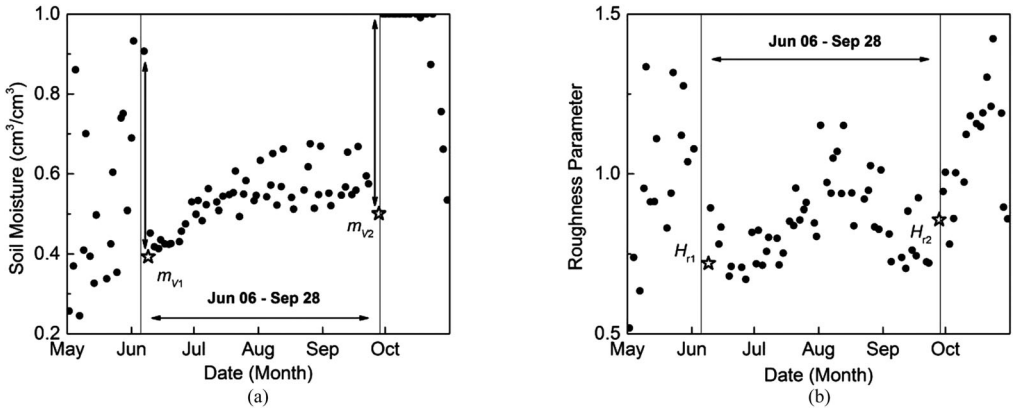

Fig. 7. (a) Time series of retrieved values of the soil moisture and (b) roughness parameter from May to October, 2013. Asterisks in the panel (a) are depicted the first and last retrieved values of the soil moisture after m_{V1} and before m_{V2} their sharp jumps (depicted vertical arrows), respectively. The corresponding values of roughness parameter, H_{r1}, H_{r2}, are depicted asterisks in the panel (b).

depth, and soil temperature were retrieved, by using the constant values of the gravimetric soil moisture, which were retrieved at the first step. Obtained in this way, the values of the volumetric soil moisture ($m_V = \rho_d \cdot m_g$) and roughness parameter are presented in Fig. 7.

The corresponding values of the retrieved soil temperature are depicted in Fig. 8 for the summer period from June 6 to September 28. Because the soil permittivity, and hence, the soil emissivity, of frozen soil weakly depends on the soil moisture (when the soil moisture is higher than 0.32 g/g, which is typical for the Arctic tundra soils) and strongly depends on the soil temperature (see Fig. 6), on the third step, the soil temperature for frozen soil was retrieved. In the winter, the soil dielectric model [7] correctly describes the complex permittivity and the quantitative ratio of ice and unfrozen water in the frozen soil in the process of decreasing and increasing the soil temperature for a given initial volumetric soil moisture, when soil is thawed. Based on these assumptions, when minimizing the norm (2), the optical depth and the soil temperature are retrieved, by using constant values of the volumetric soil moisture and roughness parameter. From January 1 to June 5, the soil temperature was retrieved using values for the soil moisture and roughness parameter equal to $m_{V1} = 0.39$ cm^3/cm^3 and $H_{r1} = 0.72$, respectively (see Fig. 7, asterisks). From September 29 to December 31, the soil temperature was retrieved using values for the soil moisture and roughness parameter equal to $m_{V2} = 0.50$ cm^3/cm^3 and $H_{r2} = 0.86$, respectively (see Fig. 7, asterisks).

V. Results and Discussion

The retrieved values for the soil moisture, roughness parameter, and optical depth spanning periods from January 1 to June 5 and from September 29 to December 31 exhibited a significant standard deviation. For the period from January 1 to June 5, the values for the soil moisture, roughness parameter, and optical depth had a mean value and a standard deviation of $m_V = 0.33 \pm 0.20$ cm^3/cm^3, $H_r = 0.59 \pm 0.38$, $\tau = 0.11 \pm 0.08$, respectively. For the period from September 29 to December 31, the retrieved values for the soil moisture, roughness parameter, and optical depth had a mean value and standard deviation of $m_V = 0.50 \pm 0.27$ cm^3/cm^3 and $H_r = 0.89 \pm 0.32$, $\tau = 0.09 \pm 0.07$, respectively. The mean values for the soil moisture and roughness parameter when the soil was frozen were close to the values of the soil moisture and roughness parameter when the soil was thawed close to the off-season (see Fig. 7, asterisks).

For the period from June 6 to September 28, the mean value and standard deviation of the values for the soil moisture, roughness parameter, and optical depth were determined to be: $m_V = 0.54 \pm 0.07$ cm^3/cm^3, $H_r = 0.83 \pm 0.13$, and $\tau = 0.03 \pm 0.02$, respectively (see Fig. 7). Large variations of the determined H_r parameter were likely associated with the implementation of the minimization algorithm of the function (2). In the process, solutions of the optimization problem using the function (2), the H_r values were determined to minimize the difference between the measured and the calculated BT. Because the area covered by an SMOS pixel (43 $\times$ 43 km) contains a wide variety of soil surface types with varying degrees of small-scale irregularities, and taking into account that for each day the SMOS observations of the BT has a unique set of observation angles with a corresponding unique set of azimuth angles, the roughness parameters had considerable deviations. The mean value of the soil moisture (0.54 cm^3/cm^3) determined using our method [see Fig. 7(a)] is 1.5 times greater than the SMOS [0.27 cm^3/cm^3, see Fig. 3(a)] and GCOM-W1 [0.33 cm^3/cm^3, see Fig. 3(b)] soil moisture data products. The soil moisture value determined using our method, treated as a parameter of the model (1), was to minimize the function (2). Currently, measurements of the soil moisture in the organic-rich soils were performed with a significant bias (from -0.092 to 0.057 m^3/m^3) [32]. Therefore, a validation of the soil moisture values determined from the ground-based weather station data is needed. Retrieved and *in situ* measured soil temperatures from 2013 are depicted in Fig. 8.

When minimizing the norm (2) in the periods when the soil temperature varied near 0 °C [see Fig. 8(a)], the RMSE between the modeled and measured multiangular BT data was greater than 6 K, and the retrieved values of soil temperature were rejected.

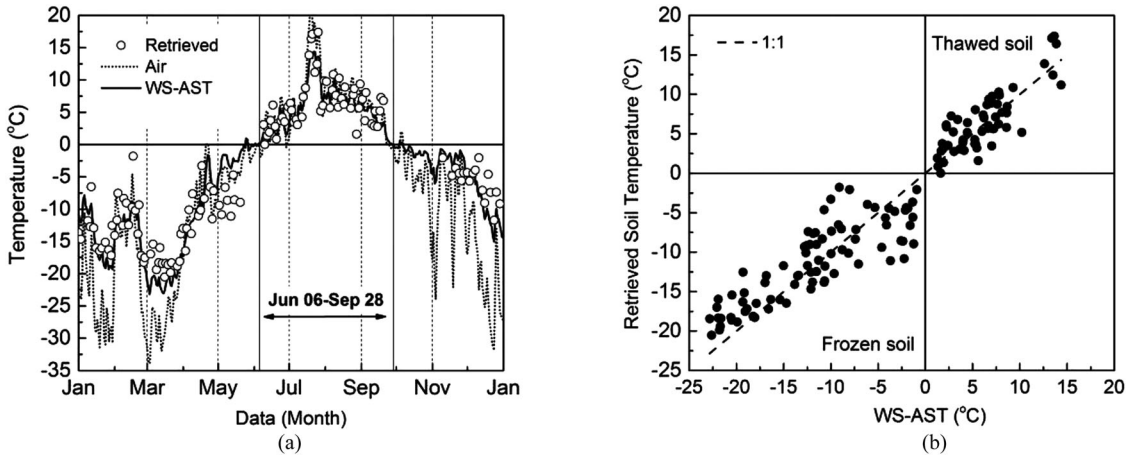

Fig. 8. (a) Time series of averaged daily air temperatures, averaged daily soil temperatures measured by WS, and retrieved soil temperature during 2013. (b) Determination coefficient between retrieved soil temperature and daily averaged soil temperatures. The calculated RMSE values are 2.2 and 3.5 °C, respectively for thawed and frozen soil conditions. The calculated determination coefficient values are 0.70 and 0.52, respectively for thawed and frozen soil conditions.

Further correlation analysis was conducted separately for the soil temperature less than and greater than 0 °C. At values of soil temperature near zero, the correlation analysis was not performed [see Fig. 8(b)]. In the summer time from June 6 to September 28, when the soil was thawed, the RMSE and determination coefficient between the retrieved soil temperatures and the weather station measurements were observed to be 2.2 °C and 0.70, respectively. In the winter, when the soil was frozen, the RMSE and determination coefficient between the retrieved soil temperatures and the weather station measurements were observed to be 3.5 °C and 0.52, respectively. The error of soil temperature measurement in the summer appeared to be less than in the winter. Apparently, these errors arose from the fact that the model (1) did not take into account the layered structure of the soil in the cases when there is a primary frozen layer over a thin thawed layer and vice versa. The presence of such a frozen (thawed) layer can produce significant variations of BT up to 100 K [33]. The layered structure of the soil when freezing and thawing can be taken into account in the model (1) by introducing the profile of the complex dielectric constant of the topsoil as done in [4] and [34]. The Fresnel reflection coefficients and the soil temperature in (1) will be calculated as reflection coefficients and the effective soil temperature of a multilayer topsoil.

The deviation of the retrieved values of the soil temperature (see Fig. 8) may be due to the approximate nature of the model (1), which does not take into account the refraction and scattering microwaves in the snowpack and the canopy. The absorption emission in the snowpack using the parameter of optical thickness in the model (1) does not completely describe the physical processes of additional emission in a layered structure of moistened snowpack when melting, and fully does not take into account the phenomenon of refraction. The impact of a snow pack on the L-band BT can be taken into account by introducing a layered structure similar to the approach described in [37]. In this case, the layered structure of the snow cover can be defined by means of the snow pack thickness and the vertical profiles of the density, temperature, and moisture of the snow. The dielectric constant of each layer in the snow pack can be estimated using a model [38]. In this case, instead of the Fresnel reflection coefficient (from the interface between the lower snow layer and the soil) used in the emission model [37], the model of the reflection coefficient from a rough soil surface used in the formula (1) can be used. For a dry snow pack, the layered structure can be simplified and represented by a dielectric layer over the ground, as in [35].

To determine the soil temperature in frozen conditions, the proposed approach was based on using fixed values of the soil moisture obtained when the soil was thawed. However, as seen in Fig. 6, in the range of soil temperature (−3–0 °C), if the soil moisture increases, then the soil permittivity increases several times and, hence, the emissivity of the frozen soil. Such an assumption is also a source of error in the method. Furthermore, the model (1) does not taken into account the variety of soil types, different vegetation covers, and the presence of water within the SMOS footprint. The fraction of the various types of soil and water bodies within the SMOS footprint can be taken into consideration by using maps of water bodies and soil types in conjunction with the temperature-dependent dielectric models for organic [6]–[8], [36] and mineral [36], [39], [40] soils. In this case, the integral BT is calculated as a superposition of the BTs in different types of soils and water bodies in accordance with percentage of area occupied by these objects in the SMOS footprint. Different vegetation covers can be accounted, if the model (1) will be complicated by introducing a vegetation scattering parameter and polarization correction factor for parameterizing the effect of the vertical and horizontal vegetation structure on the optical depth parameter using equations from [26].

The relatively low error of the soil temperature retrieval (<4 °C) suggests the possibility of applicability of the simplified model (1) for the selected test site, and disregard of these objects is already contained in the obtained error of soil temperature retrieval. If in the model (1), the influence of these objects on the radiobrightness temperature would be taken into account, reducing the error of soil temperature retrieval is possible.

Finally, to determine the soil temperature in the summer, additional independent data for air temperature were used, which may not always be available due to 1) the limited number of land-based weather stations, and 2) the limits of the IRs products (similar MODIS LST) in different weather and cloud conditions.

VI. Conclusion

The primary objective of this paper was to conduct an experimental testing of the method theoretically determined in [4] for measuring the soil temperature in an arctic tundra topsoil, using the full-polarimetric multiangular SMOS BT observation at a frequency of 1.4 GHz. The experimental validation of the proposed retrieval method was conducted with the use of SMOS BT data over a test site on the Yamal Peninsula spanning the period of January 1, 2013 to December 31, 2013. The results of the research indicate the perspectives of using the full-polarimetric multiangular BT observations in the L-band for the purpose of measuring the soil temperature in the Arctic region. As follows from the requirements for the research product of the LST retrieval using the GCOM-W1 [41], the accuracy goal for soil temperature measurements is ± 4 K. The preliminary results obtained in this study showed that these accuracy requirements were attainable for the purposes of soil temperature measurements using a microwave radiometer. The RMSE and the determination coefficient between the retrieved and measured soil temperature were found to be equal to 3.0 °C and 0.91 for the year.

For the proposed method of soil temperature retrieval, a potential for improving the simple model (1) exists by taking into account the additional factors, which could not be introduced in the BT model used. The following most significant factors have to be included to improve the model: 1) the effects of open water objects and soils types, and 2) a more accurate account of the impact of the snow pack and vegetation cover. However, the simple model of soil emission used, which does not take into account the above factors, yields promising results for the cases when: the type of soil is known and the created dielectric model corresponds to this soil type, the landscape is typical arctic tundra with dwarf shrubs with heights less than 40 cm, and the fraction of water bodies in the SMOS footprint is not greater than 7.6%.

The proposed approach needs to be modified and tested for a longer time period and for a more representative amount of ground-based test sites in the Arctic region. For this purpose, areas can be selected on the northern slope of Alaska, which is a network of weather stations at Toolik Lake, Happy Valley, Sagwon, Franklin Bluffs, and Deadhorse, which are a part of the North American Arctic transect. This Arctic area is very suitable to validate the retrieval algorithms of the soil moisture and temperature because for a long time, these weather stations measured the detailed profiles of moisture and temperature in the active layer of the soil (0–1 m), air and vegetation layer or snow pack temperatures, and the types of soils and vegetation at the weather stations area are systematized and described.

References

[1] S. Hachem, C. R. Duguay, and M. Allard, "Comparison of MODIS-derived land surface temperatures with ground surface and air temperature measurements in continuous permafrost terrain," *Cryosphere*, vol. 6, pp. 51–69, 2012, doi: 10.5194/tc-6-51-2012.

[2] L. A. Jones, J. S. Kimball, K. C. McDonald, S. T. K. Chan, E. G. Njoku, and W. C. Oechel, "Satellite microwave remote sensing of boreal and arctic soil temperatures from AMSR-E," *IEEE Trans. Geosci. Remote Sens.*, vol. 45, no. 7, pp. 2004–2018, Jul. 2007.

[3] S. Zhao, L. Zhang, T. Zhang, Z. Hao, L. Chai, and Z. Zhang, "An empirical model to estimate the microwave penetration depth of frozen soil," in *Proc. IEEE Int. Geosci. Remote Sens. Symp.*, 2012, pp. 4493–4496.

[4] V. L. Mironov, K. V. Muzalevskiy, and I. V. Savin, "Retrieving temperature gradient in frozen active layer of arctic tundra soils from radiothermal observations in L-Band—Theoretical modeling," *IEEE J. Select. Topics Appl. Earth Observ. Remote Sens.*, vol. 6, no. 3, pp. 1781–1785, Apr. 2013.

[5] J. Wigneron *et al.*, "Evaluating an improved parameterization of the soil emission in L-MEB," *IEEE Trans. Geosci. Remote Sens.*, vol. 49, no. 4, pp. 1177–1189, Apr. 2011.

[6] V. L. Mironov, R. D. De Roo, and I. V. Savin, "Temperature-dependable microwave dielectric model for an arctic soil," *IEEE Trans. Geosci., Remote Sens.*, vol. 48, no. 6, pp. 2544–2556, Jun. 2010.

[7] V. L. Mironov, I. V. Savin, and K. V. Muzalevskiy, "A temperature-dependent multi-relaxation spectroscopic dielectric model for thawed and frozen organic soil at 0.05–15 GHz," in *Proc. IEEE Int. Geosci. Remote Sens. Symp.*, Jul. 26–31, 2015, pp. 2031–2034.

[8] V. Mironov and I. Savin, "A temperature-dependent multi-relaxation spectroscopic dielectric model for thawed and frozen organic soil at 0.05–15 GHz," *Phys. Chem. Earth, A/B/C*, vol. 83, pp. 57–64, Mar. 14, 2015.

[9] Permarfrost Laboratory University of Alaska. (2015). [Online]. Marresale Database. Available: http://permafrost.gi.alaska.edu/site/ms1(/ms2, /ms3, /ms5)

[10] NOAA's National Centers for Environmental Information. (2015). [Online]. WMO Weather Station Database. Available: ftp://ftp.ncdc.noaa.gov/pub/data/gsod/

[11] [Online]. Available: http://www.arcticatlas.org/maps/catalog/

[12] A. V. Pavlov, "Active layer monitoring in northern West Siberia," presented at the Permafrost 7th Int. Conf., Yellowknife, NT, Canada, Jun. 23–27, 1998.

[13] FAO/IIASA/ISRIC/ISSCAS/JRC, Harmonized World Soil Database (version 1.2), 2012. Rome, Italy: FAO, and Laxenburg, Austria: IIASA.

[14] D. A. Walker *et al.*, "Spatial and temporal patterns of greenness on the Yamal Peninsula, Russia: Interactions of ecological and social factors affecting the Arctic normalized vegetation index," *Environ. Res. Lett.*, vol. 4, 2009, Art. no. 045004, doi: 10.1088/1748-9326/1084/1084/045004.

[15] Y. H. Kerr *et al.*, "The SMOS mission: New tool for monitoring key elements of the global water cycle," Proc. IEEE, vol. 98, no. 5, pp. 666–687, May 2010.

[16] Centre Aval de Traitement des Données SMOS. (2015). SMOS Products Dissemination Service [Online]. Available: http://www.catds.fr/sipad/

[17] NASA Jet Propulsion Laboratory. (2015). Algorithm Theoretical Basis Documents [Online]. Available: https://smap-archive.jpl.nasa.gov/files/smap2/L2&3_SM_P_RevA_web.pdf

[18] SMAP Handbook. (2014). [Online]. Available: http://smap.jpl.nasa.gov/system/internal_resources/ details/original/178_SMAP_Handbook_FINAL_1_JULY_2014_Web.pdf

[19] A. Basharinov and A. Shutko, "Simulation studies of the SHF radiation characteristics of soils under moist conditions," NASA Tech. Transl. TT F-16, 1975.

[20] GCOM-W1 Data Providing Service. (2015). Search Product [Online]. Available: http://gcom-w1.jaxa.jp/

[21] R. Muskett, V. Romanovsky, W. Cable, and A. Kholodov, "Active-Layer soil moisture content regional variations in Alaska and Russia by ground-based and satellite-based methods, 2002 through 2014," *Int. J. Geosci.*, vol. 6, no. 1, pp. 12–41, 2015.

[22] M. Schwank *et al.*, "Snow density and ground permittivity retrieved from L-band radiometry: A synthetic analysis," *IEEE J. Select. Topics Appl. Earth Observ. Remote Sens.*, vol. 8, no. 8, pp. 3833–3845, Aug. 2015.

[23] C. André, C. Ottlé, A. Royer, and F. Maignan, "Land surface temperature retrieval over circumpolar Arctic using SSM/I–SSMIS and MODIS data," *Remote Sens. Environ.*, vol. 162, pp. 1–10, 2015.

[24] S. Westermann, M. Langer, and J. Boike, "Systematic bias of average winter-time land surface temperatures inferred from MODIS at a site on Svalbard, Norway," *Remote Sens. Environ.*, vol. 118, pp. 162–167, 2012.

[25] M. Langer, S. Westermann, and J. Boike, "Spatial and temporal variations of summer surface temperatures of wet polygonal tundra in Siberia—Implications for MODIS LST based permafrost monitoring," *Remote Sens. Environ.*, vol. 114, no. 9, pp. 2059–2069, 2010.
[26] J. P. Wigneron, Y. H. Kerr, P. Waldteufel, K. Saleh, M.-J. Escorihuela, P. Richaume, P. Ferrazzoli, P. de Rosnay, R. Gurney, J. C. Calvet, J. P. Grant, M. Guglielmetti, B. Hornbuckle, C. Matzler, T. Pellarin, and M. Schwank, "L-band microwave emission of the biosphere (L-MEB) model: Description and calibration against experimental data sets over crop fields," *Remote Sens. Environ.*, vol. 107, pp. 639–655, 2007.
[27] H. Lawrence, J.-P. Wigneron, F. Demontoux, A. Mialon, and Y. H. Kerr, "Evaluating the semiempirical H–Q model used to calculate the L-band emissivity of a rough bare soil," *IEEE Trans. Geosci. Remote Sens.*, vol. 51, no. 7, pp. 4075–4084, Jul. 2013.
[28] A. Mialon, L. Coret, Y. H. Kerr, F. Secherre, and J.-P. Wigneron, "Flagging the topographic impact on the SMOS signal," *IEEE Trans. Geosci. Remote Sens.*, vol. 46, no. 3, pp. 689–694, Mar. 2008.
[29] N. Ye, J. P. Walker, J. Guerschman, D. Ryu, and R. J. Gurney, "Standing water effect on soil moisture retrieval from L-band passive microwave observations," *Remote Sens. Environ.*, vol. 169, pp. 232–242, 2015.
[30] K. Rautiainen *et al.*, "L-band radiometer observations of soil processes in boreal and subarctic environments," *IEEE Trans. Geosci. Remote Sens.*, vol. 50, no. 5, pp. 1483–1497, May 2012.
[31] V. L. Mironov, S. A. Komarov, Y. I. Lukin, and D. S. Shatov, "A technique for measuring the frequency spectrum of the complex permittivity of soil," *J. Commun. Technol. Electron.*, vol. 55, no. 12, pp. 1368–1373, 2010.
[32] S. Bircher, N. Skou, K. H. Jensen, J. P. Walker, and L. Rasmussen, "A soil moisture and temperature network for SMOS validation in Western Denmark," *Hydrol. Earth Syst. Sci.*, vol. 16, pp. 1445–1463, 2012, doi: 10.5194/hess-16-1445-2012.
[33] P. P. Bobrov, S. V. Krivaltsevich, V. L. Mironov, and A. S. Jaschenko, "The effect of frozen soil layer thickness on thermal emission at the wavelength 3.6–11 cm," *Russian Phys. J.*, vol. 49, no. 9, pp. 907–912, 2006.
[34] P. P. Bobrov, V. L. Mironov, and A. S. Yashchenko, "Diurnal dynamics of soil brightness temperatures observed at frequencies of 1.4 and 6.9 GHz in the processes of freezing and thawing," *J. Commun. Technol. Electron.*, vol. 55, no. 4, pp. 395–402, 2010.
[35] M. Schwank *et al.*, "Snow density and ground permittivity retrieved from l-band radiometry: A synthetic analysis," *IEEE J. Select. Topics Appl. Earth Observ. Remote Sens.*, vol. 8, no. 8, pp. 3833–3845, Aug. 2015.
[36] K. V. Muzalevskiy and L. Yury, "Effects of organo-mineral structure of arctic topsoil on the own thermal radiation in the L-band," in *Proc. Int. Siberian Conf. Control Commun.*, Omsk, Russia, 2015, pp. 1–4.
[37] J. Lemmetyinen, J. Pulliainen, A. Rees, A. Kontu, Q. Yubao, and C. Derksen, "Multiple-layer adaptation of HUT snow emission model: Comparison with experimental data," *IEEE Trans. Geosci. Remote Sens.*, vol. 48, no. 7, pp. 2781–2794, Jul. 2010.
[38] M. Tiuri, A. Sihvola, E. Nyfors, and M. Hallikaiken, "The complex dielectric constant of snow at microwave frequencies," *IEEE J. Ocean. Eng.*, vol. 9, no. 5, pp. 377–382, Dec. 1984.
[39] V. L. Mironov and S. V. Fomin, "Temperature dependable microwave dielectric model for moist soils," in *Proc. PIERS*, Beijing, China, Mar. 23–27, 2009, pp. 831–835.
[40] V. L. Mironov, I. P. Molostov, and V. V. Scherbinin, "Dielectric model of a mineral arctic soil thawed and frozen at 0.05–15 GHz," in *Proc. Int. Siberian Conf. Control Commun.*, Omsk, Russia, 2015, pp. 1–7.
[41] Global change observation mission-Water (GCOM-W1). (2015). Data products [Online]. Available: http://suzaku.eorc.jaxa.jp/GCOM_W/data/data_w_product-3.html

Konstantin Viktorovich Muzalevskiy received the M.S. degree in radio science and electronics from Altai State University, Altai Krai, Russia, in 2004, and the Ph.D. degree in radiophysics from the Kirensky Institute of Physics Siberian Branch of the Russian Academy of Sciences (SB RAS), Krasnoyarsk, Russia, in 2010.

Since 2008, he has been an Assistant Professor at the M. F. Reshetnev Siberian State Aerospace University, Krasnoyarsk. Since 2010, he has been a Research Fellow at the Laboratory of Radiophysics of Remote Sensing, Kirensky Institute of Physics SB RAS. His work was supported by the Krasnoyarsk Regional Foundation for Support of Scientific and Technological Activities (2010, 2011, 2015), The Mikhail Prokhorov Foundation (2010), Foundation for Assistance to Small Innovative Enterprises in Science and Technology Grant (2009), and Russian Foundation for Basic Research (2009, 2012) as a young Scientist. He is the Leader of the youth projects devoted to developing the remote sensing technologies of soil temperature and soil moisture monitoring in the Arctic tundra regions during freezing and thawing process. He is the author/coauthor of more than 40 scientific publications and a book.

Zdenek Ruzicka received the Master's degree in geoinformatics from Czech Technical University, Prague, Czech Republic, in 2012.

He is currently an Engineer Researcher at the Kirensky Institute of Physics, Siberian Branch of the Russian Academy of Sciences, Krasnoyarsk, Russia, and a postgraduate at Siberian State Aerospace University, Krasnoyarsk. His research interests include geoinformatics and processing of remote sensing data.